Injectable Sustained Release Microparticles of Curcumin: A New Concept for Cancer Chemoprevention

Komal Shahani[a,b], **Suresh Kumar Swaminathan**[b], **Diana Freeman**[c], **Angela Blum**[c], **Linan Ma**[d], and **Jayanth Panyam**[b,d,*]

[a]Department of Pharmaceutical Sciences, Eugene Applebaum College of Pharmacy and Health Sciences, Wayne State University, Detroit, MI 48201

[b]Department of Pharmaceutics, College of Pharmacy, University of Minnesota, Minneapolis, MN 55455

[c]Research Animal Resources, Academic Health Center, University of Minnesota, Minneapolis, MN 55455

[d]Masonic Cancer Center, University of Minnesota, Minneapolis, MN 55455

Abstract

Poor oral bioavailability limits the use of curcumin and other dietary polyphenols in the prevention and treatment of cancer. Minimally invasive strategies that can provide effective and sustained tissue concentrations of these agents will be highly valuable tools in the fight against cancer. The objective of this study was to investigate the use of an injectable sustained release microparticle formulation of curcumin as a novel approach to breast cancer chemoprevention. A biodegradable and biocompatible polymer, poly(D,L-lactide-*co*-glycolide) (PLGA), was used to fabricate curcumin microparticles. When injected subcutaneously in mice, a single dose of microparticles sustained curcumin levels in the blood and other tissues for nearly a month. Curcumin levels in the lungs and brain, frequent sites of breast cancer metastases, were 10-30-fold higher than that in the blood. Further, curcumin microparticles showed marked anticancer efficacy in nude mice bearing MDA-MB-231 xenografts compared to other controls. Repeated systemic injections of curcumin were not effective in inhibiting tumor growth. Treatment with curcumin microparticles resulted in diminished VEGF expression and poorly developed tumor microvessels, indicating a significant effect on tumor angiogenesis. These results suggest that sustained delivery of chemopreventives such as curcumin using polymeric microparticles is a promising new approach to cancer chemoprevention and therapy.

Keywords

Polyphenols; Polymeric Systems; Sustained Release; Bioavailability; Chemoprevention

Introduction

Curcumin, a dietary polyphenol derived from the root of *Curcuma longa* Linn., has demonstrated significant potential as a chemopreventive, with beneficial effects in all the three stages of carcinogenesis (1). Curcumin exerts its antitumor effect by modulating the expression of multiple genes involved in tumor proliferation, apoptosis, invasion, and angiogenesis (2). Despite its efficacy and safety, the clinical usefulness of curcumin is diminished by its poor

*Author for correspondence: Department of Pharmaceutics, College of Pharmacy, University of Minnesota, Minneapolis, MN 55455, Phone: 612-624-0951, Fax: 612-626-2125, jpanyam@umn.edu.

oral absorption and extensive hepatic first pass metabolism, resulting in low oral bioavailability (< 1%) (3). Several studies suggest that oral consumption may not furnish adequate tissue levels of curcumin necessary for effective cancer prevention and treatment (4-8).

Previous pre-clinical studies have used repeated systemic injections of curcumin to overcome poor oral bioavailability (9,10). However, this is not a clinically feasible approach to chemoprevention. The current study is the first to report the use of an injectable, sustained release formulation, which, after a single dose, results in near-constant systemic concentrations of curcumin for several weeks and a significant inhibition of tumor growth in an orthotopic mammary tumor model. Further, the results of the study show that sustained low levels of curcumin achieved with microparticles may elicit certain antitumor effects not observed after repeated systemic injections.

Materials and Methods

Materials

Curcumin (minimum 94% curcuminoid content) and polyvinyl alcohol (average M_W 30-70 kDa; PVA) were purchased from Sigma (St. Louis, MO). Poly(D,L-lactide-*co*-glycolide) (lactide-to-glycolide ratio of 50:50 and average M_W of ~120 kDa; PLGA) was from Durect Corporation (Pelham, AL). Six-well Transwell® inserts were purchased from Corning (Lowell, MA). CellTiter 96® aqueous non-radioactive cell proliferation assay (MTS) kit was purchased from Promega (Madison, WI). Monoclonal rat anti-mouse Ki-67 antibody was from Dako (Carpinteria, CA). Polyclonal goat anti-mouse platelet/endothelial cell adhesion molecule-1 (PECAM-1 CD31) antibody was from Santa Cruz Biotechnology (Santa Cruz, CA), while polyclonal rabbit anti-human cleaved caspase-3 (Asp 175) antibody was from Cell Signaling Technology (Beverly, MA). For Western blotting, antibodies against cyclin D1 (M-20), cyclooxygenase-2 (COX-2; H-62), matrix metalloproteinase-9 (MMP-9; H-129) and vascular endothelial growth factor (VEGF; 147) were purchased from Santa Cruz Biotechnology, and antibody against β-tubulin was from Cell Signaling Technology.

Cell lines

MDA-MB-231 cells, stably transfected with luciferase, were purchased from Caliper Life Sciences (Hopkinton, MA). 4T1, MCF-7, and EMT-6 cells were purchased from American Type Culture Collection (Manassas, VA).

Formulation of curcumin-loaded PLGA microparticles

Curcumin microparticles were prepared using a modification of emulsion-solvent evaporation technique (11,12). Curcumin (20 mg) and PLGA (20 mg) were solubilized in chloroform (1.5 ml) and methanol (0.15 ml). This solution was emulsified into 2% w/v aqueous PVA solution (6 ml) by vortex mixing (Digital Vortex Mixer, VWR, West Chester, PA) at 1000 rpm for 2 min. The emulsion formed was subjected to high vacuum (710 mm Hg) at 4° C using a rotary evaporator (Laborta 4001 Efficient Rotaevaporator, Heidolph, Germany), which resulted in rapid removal of the organic solvents. Microparticles were recovered by centrifugation (5810R, Eppendorf, Westbury, NY) at 1000 rpm for 10 min, washed twice with 10% w/v Tween 80 in endotoxin-free water (50 ml), then twice with endotoxin-free water (50 ml), and lyophilized (Freezone 4.5®, Labconco, Kansas City, MO).

Microparticle characterization

Mean diameter of microparticles was determined using optical microscopy. Microparticles (~1 mg) were dispersed in 0.5 ml distilled water by sonication (Model 3000, Misonix, Farmingdale, NY) at 3 watts for 60 sec. A drop of this dispersion was placed on a glass slide and observed

under a microscope (Eclipse TS100, Nikon Instruments, Melville, NY) at 400X magnification. Diameters of 500 particles in several different fields were measured using Adobe Photoshop (Adobe Systems, San Jose, CA), and the number average particle diameter was calculated. The morphology of microparticles was examined using field emission scanning electron microscopy (SEM). Microparticles were placed on a double stick carbon tape over aluminum stubs and carbon coated. The coated samples were observed under an electron microscope (JSM 6500F, JEOL, Peabody, MA) at 1500X magnification. To determine drug loading, microparticles (2 mg) were extracted with 2 ml methanol for 18 h (Labquake Shaker, Barnstead Thermolyne, Dubuque, IA). The methanolic extract was centrifuged at 13,500 rpm for 15 min and curcumin concentration in the supernatant was quantified by HPLC (System Gold® 126 Solvent Module and 508 Autosampler, Beckman Coulter, Fullerton, CA) using a C-18 column (Ultrasphere ODS, 250 mm × 4.6 mm i.d., 5 µm particle size, Beckman). A 60/40 mixture of acetonitrile and ammonium acetate (10 mM, pH 4) was used as mobile phase at a flow rate of 1 ml/min. Curcumin was detected using a PDA detector (System Gold® 168 Detector) at a wavelength of 430 nm. The retention time of curcumin under these conditions was 5.8 min. Drug loading in microparticles (% w/w) was defined as the amount of curcumin in 100 mg of microparticles.

In vitro release of curcumin from microparticles

The release study was done in a 6-well plate containing Transwell® inserts with a pore size of 400 nm. Phosphate buffered saline (0.15 M, pH 7.4; PBS) containing 10% w/v Tween 80, 0.1% w/v n-acetyl cysteine, and 0.01% w/v butylated hydroxytoluene was used as the release buffer. Curcumin-loaded microparticles (equivalent to 2 µg curcumin), suspended in 1 ml of the release buffer, were placed on top of the Transwell® insert and 3 ml of the release buffer was added to the bottom of the well. The 6-well plates with the inserts were sealed with parafilm, and placed in an incubator shaker (C24 Incubator Shaker, New Brunswick Scientific, Edison, NJ) set at 100 rpm and 37° C. At various time intervals, the entire release buffer in the bottom chamber was removed and replaced with fresh release buffer. Curcumin concentration in the release buffer was quantified by HPLC. The composition of the release buffer was optimized to ensure that curcumin released from microparticles was soluble and stable in the buffer. A control experiment performed with curcumin solution (instead of microparticles) confirmed rapid (< 8 h) equilibration of curcumin between the two chambers.

Inflammatory response to microparticles in mice

All animal experiments were carried out in compliance with protocols approved by the Institutional Animal Care and Use Committees at Wayne State University and the University of Minnesota. Six week old female BALB/c mice (Charles River Laboratories, Wilmington, MA) were injected subcutaneously with a single dose of curcumin-loaded microparticles or blank microparticles. Untreated animals were used as negative controls. Subcutaneous tissue from the vicinity of the injection site was collected after 48 h, fixed in 10% phosphate buffered formalin, embedded in paraffin, and sectioned. After deparaffinization, sections were stained with hematoxylin-eosin (H & E). For each sample, large, darkly-stained nuclei, indicating the presence of inflammatory cells (13), were counted from 10 different fields under an optical microscope at 400X magnification. Results were expressed as the average number of inflammatory cells/field.

Curcumin pharmacokinetics in mice

For evaluating curcumin kinetics following a single intraperitoneal (IP) injection, mice were injected with curcumin (2.2 mg) dissolved in 0.05 ml of a 50/50 mixture of polyethylene glycol (PEG) 400 and 95% ethanol. Animals were euthanized at various time points (n = 6 per time point), and blood samples were collected and analyzed for curcumin concentration. To

determine curcumin kinetics following multiple IP injections, mice were injected with curcumin (2.2 mg) on days 1, 3, and 6. Animals were euthanized, and tissue samples were collected at 30 min (day 1), 24 h, 48 h, 72 h and 144 h post injection (n=6-9 per time point). To determine curcumin kinetics following microparticle administration, mice were injected with a single dose of curcumin-loaded microparticles in the subcutaneous space near the neck. Microparticles (equivalent to 29.1 mg curcumin) were dispersed in 0.5 ml PBS prior to injection. Animals were euthanized at various time points (n = 6-7 per time point), and tissue samples were analyzed for curcumin concentration. For drug analysis, tissue samples were homogenized in 2 ml distilled water, lyophilized, and extracted with 2 ml diethyl ether. Blood samples were extracted with 2 ml diethyl ether without prior processing. The ether extracts were evaporated in a water bath at 37° C and reconstituted with 0.3 ml mobile phase. Hydroxybenzophenone was used as the internal standard. Drug concentration in the extracts was determined by LC-MS/MS (Agilent 1100, Agilent Technologies, Palo Alto, CA, coupled to Finnigan TSQ Quantum Discovery Max triple quadrupole detector, Thermo Electron, San Jose, CA). Separation was achieved on a C-18 column (Zorbax SB-18, 150 mm × 0.5 mm i.d., 5 μm particle size, Agilent) using a 60/40 mixture of acetonitrile and ammonium acetate (10 mM, pH 4) as the mobile phase (flow rate 10 μl/min). Samples were analyzed in positive ion mode. Curcumin and hydroxybenzophenone were monitored using single reaction monitoring of the 369.2 to 285.1 and 199.2 to 121.1 transitions, respectively. Retention times of hydroxybenzophenone and curcumin under these conditions were 3.8 and 4.8 min, respectively. The chromatographic data were acquired and analyzed using Xcaliber software (Thermo Scientific). Curcumin concentrations were normalized to wet tissue weights. Pharmacokinetic parameters were estimated from the blood concentration-time data based on a non-compartmental model using WinNonlin (Pharsight Corporation, Mountain View, CA).

Cytotoxicity studies

Cells were seeded in 96-well plates at a seeding density of 5,000 cells/well/0.1 ml medium. Following attachment, cells were treated with 0.1-50 μM curcumin dissolved in the growth medium (using 0.1% DMSO) for 72 h. Fresh medium containing curcumin was added every day. Cell viability was measured using MTS assay. The formazan product formed was quantified by measuring the absorbance at 490 nm using a microplate reader (ELx800, BioTek Instruments, Winooski, VT). The mean absorbance for each treatment was determined, and then expressed as percent viability relative to control (0.1% DMSO treated group).

In vivo anticancer efficacy of curcumin formulations

Female BALB/c nu/nu mice (Charles River Laboratories) were used in the study. Mice were randomized into 4 groups of 6 animals each. In the first group of animals, a single dose of curcumin-loaded microparticles (equivalent to 58.2 mg curcumin) was injected in the subcutaneous space near the neck a day before the injection of tumor cells. MDA-MB-231 cells were suspended in Hanks balanced salt solution (2×10^6 cells/0.1ml/mouse) and injected into the 4th mammary fat pad of the mice. The second group of animals received an equivalent dose of blank microparticles a day prior to the injection of tumor cells. In the third group of animals, the first IP dose of curcumin (4.4 mg) was given a day before the injection of tumor cells. Subsequent doses were administered thrice a week till the end of the study. In the fourth group, animals were injected IP with the vehicle thrice a week. Tumor size was measured on alternate days throughout the study. Length (L) and width (W) of the tumor were measured using Vernier calipers and the tumor volume (V) was calculated using the formula $V = L \times W^2 / 2$, where L and W are the longest and shortest diameters, respectively. Animals were euthanized at the end of the study, and tumors were collected and frozen at −80° C.

Immunohistochemistry

Tumor samples from the above study were fixed in 10% phosphate buffered formalin for 24 h and subsequently transferred to 70% ethanol before being embedded in paraffin and sectioned. After deparaffinization, sections were stained with antibodies against CD31, Ki-67 and cleaved caspase-3. CD31 and Ki-67 positive staining was detected with appropriate biotinylated secondary antibody, followed by incubation with streptavidin-horseradish peroxidase (Vector Laboratories, Burlingame, CA) and development with diaminobenzidine (DAB; Dako). Sections were counterstained with Mayer's hematoxylin (Dako). Presence of cleaved caspase-3 was detected with EnVision system (Dako), followed by development with DAB and counterstaining with Mayer's hematoxylin. Stained slides were evaluated under an optical microscope at 400X magnification. For Ki-67 and cleaved caspase-3 staining, the percent of DAB positive cells was counted in at least 10 different fields per sample, and the results were presented as % proliferating and % apoptotic cells, respectively. Cells in the central necrotic region of the tumors were excluded from analysis. For CD31 staining, DAB positive microvessels were counted in at least 10 different fields per sample, and the results were presented as the average number of CD31 positive microvessels/field.

Western blotting

Tumors were cut into small pieces and incubated with RIPA buffer (Thermo Scientific) containing protease inhibitor cocktail (Sigma) and phosphatase inhibitor (Sigma) for 1 h on ice. Samples were sonicated at 3 watts for 30 sec on ice, further incubated for 1 h on ice, and finally centrifuged at 10,000 rpm for 10 min at 4° C. Protein concentrations in the supernatants were analyzed by BCA assay (Thermo Scientific), with bovine serum albumin as the standard. Protein samples (35-45 μg) were loaded onto 4-16% SDS-PAGE gel (Bio-Rad Laboratories, Hercules, CA) and, after electrophoresis, transferred onto a nitrocellulose membrane (Whatman, Piscataway, NJ) using a Criterion blotter (Bio-Rad). The membrane was blocked with 5% non-fat dry milk in TBST for 1 h, and incubated with primary antibodies against cyclin D1, COX-2, MMP-9, VEGF, or β-tubulin, diluted in either 5% non-fat dry milk in TBST or 5% bovine serum albumin in TBST overnight at 4° C. After three 5-min washes with TBST, the membrane was incubated with anti-rabbit IgG conjugated with horseradish peroxidase (Cell Signaling) in 5% non-fat dry milk in TBST for 1 h and then washed three times with TBST. The transferred proteins were then visualized using SuperSignal West Pico Chemiluminescent Substrate (Thermo Scientific). For densitometric quantification, immunoblots were digitized on a flat bed scanner and the signal intensities of the visualized bands were quantified using Adobe Photoshop. Relative expression was calculated by dividing the signal intensity of each band by the signal intensity of β-tubulin band in the corresponding lane.

Statistical analysis

Differences in tissue concentrations and cytotoxicities were analyzed using Student's t-test. Generalized linear mixed effect ANOVA following natural log transformation of tumor volumes was used to analyze the tumor growth inhibition data. The differences in the slopes of the tumor growth curves were tested by Bonferroni adjustment. Differences in inflammatory cell populations, percent proliferating and apoptotic cells, and microvessel density were determined using ANOVA followed by *post hoc* Dunnett's multicomparison test. A $p < 0.05$ was considered significant.

Results

Microparticle characterization and *in vitro* release of curcumin

Optical microscopy studies indicated that microparticles had an average diameter of 22 ± 9 μm. SEM studies indicated that microparticles had a smooth, spherical morphology, without

the presence of curcumin crystals on the surface (Fig. 1A). Curcumin was loaded efficiently in microparticles (38% w/w loading; 75% encapsulation efficiency). *In vitro*, microparticles sustained the release of curcumin over a six-week period (Fig. 1B). A small burst release was observed in the initial 24 h (~10%), followed by a relatively constant release over the remainder of the study (100% over 6 weeks).

Inflammatory response to curcumin microparticles

Inflammatory cells were recognized in the H & E stained sections by the presence of purple-stained, distinctively-shaped nuclei (Fig. 1C). The average number of inflammatory cells in the negative control (untreated) was 68 ± 31/field. Blank microparticles induced a significant inflammatory response (208 ± 24 cells/field; $p < 0.05$); however, the inflammatory response was significantly less in the presence of curcumin microparticles (124 ± 26 cells/field; $p < 0.05$ Vs blank microparticles).

Curcumin pharmacokinetics following IP injections and microparticles

A single IP injection of curcumin solution resulted in biphasic clearance of curcumin from the blood (elimination $t_{1/2}$ ~6.94 h, clearance ~3 L/kg/h; Fig. 2A). Multiple IP injections resulted in peaks and troughs in the blood concentration-time profile (Fig. 2B). A single dose of microparticles sustained curcumin levels in the blood for 4 weeks (Fig. 2C). Blood concentrations were in the 0.01 - 0.1 μM range, which was similar to that seen at the end of a week following thrice a week IP administration of curcumin solution (Fig. 2B). With either treatment, curcumin concentrations in the lungs and brain were 10-30-fold higher than in the blood and were sustained through 4 weeks (Fig. 2C; data not shown for multiple IP dosing). Visual inspection of the injection site at the time of sacrifice indicated that microparticles were well localized at the site of injection (not shown). Gross necropsy revealed no signs of acute toxicity with any of the treatments.

Curcumin cytotoxicity

To determine a suitable *in vivo* tumor model for evaluating the anticancer efficacy of curcumin microparticles, an *in vitro* cytotoxicity study was conducted in different breast cancer cell lines. As shown in Fig. 3A, curcumin did not have a significant effect on MCF-7 cells at doses below 20 μM, and on 4T1 and EMT-6 cells at doses below 10 μM. Curcumin induced significant cytotoxicity ($p < 0.05$) in MDA-MB-231 cells at doses ≥ 0.1 μM in a dose-dependent manner. Based on these results, MDA-MB-231 cells were chosen for *in vivo* tumor growth inhibition studies.

In vivo anticancer efficacy of curcumin formulations

The anticancer efficacy of curcumin treatments were evaluated in nude mice bearing orthotopic MDA-MB-231 xenografts. In this tumor model, a single dose of curcumin microparticles significantly inhibited tumor growth compared to other treatments (Fig. 3B; $p < 0.05$). At the end of the study, the mean tumor volume in the curcumin microparticle treated group was 49% lower than that in the blank microparticle treated group. Repeated IP administration of curcumin solution had no effect on tumor growth compared to vehicle treatment.

Curcumin downregulates markers of angiogenesis, metastasis and proliferation, and induces apoptosis

To understand the mechanisms underlying the enhanced anticancer efficacy of curcumin microparticles, tumors were analyzed for biomarkers of angiogenesis (CD31 and VEGF) (14-17), metastasis (MMP-9) (14,15,18,19), proliferation (Ki-67 and cyclin D1) (14,15,20), and apoptosis (cleaved caspase-3 and COX-2) (14,15,21). The average microvessel density in tumors from the curcumin microparticle treated group (16.93 ± 2.45, Fig. 4) was significantly

lower ($p < 0.05$) than that in tumors from the blank microparticle treated group (27.73 ± 1.73). There was no significant difference in the microvessel density in tumors that received repeated curcumin solution (24.33 ± 1.31) or the vehicle (21.93 ± 1.19). The CD31 positive microvessels were much smaller and less well-developed in the curcumin microparticle group than those in the other groups. Treatment with curcumin microparticles and curcumin solution decreased the relative VEGF expression in tumors by 78% and 48%, respectively, compared to controls (Fig. 5). There were 57% and 11% reductions in the relative MMP-9 expression in tumors from curcumin microparticle and curcumin solution treated groups, respectively, compared to controls (Fig. 5). Curcumin microparticle treatment reduced the number of proliferating cells by 45% (Fig. 4; $p < 0.05$) and the relative cyclin D1 expression by 52% (Fig. 5) compared to blank microsphere treatment. Curcumin microparticle treatment also resulted in a 2.5-fold increase in the number of apoptotic cells relative to that with blank microparticle treatment (Fig. 4). Repeated curcumin dosing had no effect on tumor cell proliferation, apoptosis or the relative cyclin D1 expression compared to vehicle treatment (Figs. 4 and 5). There was a 1.5-fold decrease in the relative COX-2 expression in tumors from curcumin microparticle and solution treated groups compared to the respective controls (Fig. 5).

Discussion

Poor oral bioavailability of curcumin and other naturally-occurring chemopreventive agents often limits their usefulness as chemopreventive and chemotherapeutic agents (3,22,23). In a Phase I clinical trial, oral consumption of 3.6 g curcumin daily resulted in a low nanomolar (11.1 nM) plasma concentration (7). Other clinical studies confirm the low bioavailability of orally administered curcumin (6,8). Minimally invasive strategies that can provide effective and sustained tissue concentrations of curcumin will help translate the pre-clinical efficacy of curcumin to the clinic. The goal of this study was to investigate the use of a sustained release microparticle formulation of curcumin as a novel approach to chemoprevention.

PLGA polymer was selected for the fabrication of curcumin microparticles, because of its safety profile, biodegradability, and sustained release properties. PLGA microparticles are currently approved for use in other indications. Microparticles entrapping a synthetic peptide analogue of luteinizing hormone-releasing hormone, Zoladex® (Astra-Zeneca), have been approved for the palliative treatment of prostate and breast cancer (24). Similarly, microparticles containing a synthetic decapeptide analogue of luteinizing hormone-releasing hormone, Trelstar Depot® (Watson), are used for the palliative treatment of advanced prostate cancer (25). An important feature of PLGA microparticles is that the duration of drug release can be varied from a few days to several months (26-28). This allows for infrequent, patient-friendly dosing regimens. The current study showed that PLGA microparticles can efficiently encapsulate curcumin and sustain its release for several weeks.

An important concern with PLGA microparticles is the inflammatory response often observed at the site of injection (13,29). Degradation products of PLGA are lactic and glycolic acids and their soluble oligomers (30). These byproducts cause local acidity and inflammation, which can affect drug absorption from the injection site (31). In the current studies, blank PLGA microparticles caused a significant inflammatory response as expected. However, the response was significantly diminished by the presence of curcumin in microparticles. Curcumin has been shown to reduce inflammation by inhibiting a number of inflammatory mediators (32). Curcumin can modulate arachidonic acid metabolism at several targets, including inhibition of phosphorylation of cytosolic phospholipase A$_2$, inhibition of COX-2 protein expression and catalytic activity (although weakly), and inhibition of lipooxygenase (LOX) activity (33). Curcumin can bind to the active site of LOX, inhibit the enzyme activity competitively and become oxygenated (34). Similarly, curcumin has been shown to be a weak scavenger of nitric oxide (35). The current study evaluated the inflammatory response at a single time point (48

h) following microparticle administration. While previous studies have shown that peak response occurs over this time period (13,29), a more detailed study evaluating the response over a longer duration is needed to further characterize the inflammatory response to curcumin microparticles.

Pharmacokinetic studies were done to establish the blood concentrations achievable with the different formulations. The doses used in this study were selected based on previously published reports. For example, Khor et al (36) investigated thrice a week IP administration of curcumin solution (6 μmol ~ 2.2 mg curcumin/dose), which was moderately effective in inhibiting the growth of a prostate tumor xenograft. We used the same dose and dosing schedule to evaluate curcumin blood concentrations after repeated IP administration. For microparticles, the relationship between clearance (CL), rate of drug input (R_0) and steady state plasma concentration ($C_{ss} = R_0 / CL$) was used to calculate the drug release rate required to achieve a target plasma concentration of ~1 μM. The above relationship assumes a constant (zero-order) drug input. While the drug release rate from PLGA microparticles is usually not zero-order (37), *in vitro* release studies show that constant rate input is a reasonable assumption in this case. Clearance was estimated using pharmacokinetic data from the single IP dose study. Blood levels of curcumin were sustained for 4 weeks following a single dose of curcumin microparticles, which confirmed that microparticles controlled curcumin release *in vivo*. However, the blood levels were lower than the estimated 1 μM concentration. It is possible that drug release from PLGA microparticles was slower *in vivo* than *in vitro* (38). Interestingly, curcumin concentrations in the lungs and brain were significantly higher than the blood concentrations. The lungs and brain are common sites of metastases in breast cancer patients (39,40). Curcumin microparticle treatment also reduced the expression of MMP-9, an enzyme that degrades extracellular matrix and a marker for metastasis (14,18,19). Although not investigated here, the above observations suggest that curcumin microparticles could be highly effective against breast cancer metastases. Tissue levels at time points beyond 4 weeks were not determined as curcumin concentrations (especially in the blood) were expected to be below the detection limit of the analytical technique.

Based on the magnitude of tissue concentrations achieved with curcumin microparticles and the results of the cytotoxicity study in different cell lines, MDA-MB-231 cells were selected for the *in vivo* efficacy studies. The tumor growth inhibition study demonstrated the anticancer efficacy of curcumin microparticles. Antitumor effect of curcumin has been linked to inhibition of tumor cell proliferation and induction of apoptosis (36,41). COX-2 plays an important role in promoting tumor cell proliferation and in suppressing apoptosis (42). Curcumin has been shown to reduce COX-2 expression through downregulation of NF-κB activation (43). Cyclin D1, a component subunit of cyclin-dependent kinase (CDK) 4 and CDK 6, is rate-limiting factor in the progression of cells through the first gap (G1) phase of the cell cycle (44). Curcumin suppresses cyclin D1 expression through downregulation of NF-κB activation (45, 46). In addition, curcumin induces apoptosis through downregulation of Bcl-2 and Bcl-X_L, upregulation of Bax and Bad, induction of cytochrome c release, activation of cleaved caspase-3, and cleavage of PARP (47,48). Correlating with enhanced inhibition of tumor growth, curcumin microparticle treatment resulted in downregulation of markers of cell proliferation and in greater induction of apoptosis compared to other groups.

Treatment with curcumin microparticles had a significant effect on tumor angiogenesis. Previous studies have shown that curcumin suppresses NF-κB induced VEGF expression, resulting in decreased angiogenesis (49). While there is currently no evidence in the literature, it is possible that curcumin also interacts with VEGF physico-chemically to inhibit its binding to its receptor. CD31, an adhesion molecule expressed by microvascular endothelial cells, has been used a biomarker of tumor angiogenesis (16,17). Treatment with curcumin microparticles resulted in fewer and less well-developed CD31 positive microvessels compared to a large

number of darkly stained and intact vessels in other groups. VEGF expression in the curcumin microparticle treated group was also lower than that in the other groups, which correlates well with diminished angiogenesis observed in this group.

It was surprising to note that, despite resulting in high tissue concentrations, repeated IP dosing was not effective in inhibiting tumor growth. It is possible that continuous exposure to low concentrations of curcumin following microparticle treatment may elicit certain pharmacological effects, which are not observed after repeated IP dosing of curcumin solution. Similar variability in therapeutic response, depending on the dose and the kinetics of drug exposure, has been observed for curcumin and other drugs. Kang et al. (50) reported a significant decrease in the cellular reactive oxygen species (ROS) levels in human hepatoma Hep3B cells treated with low doses (10-20 μM) of curcumin. At higher doses, however, curcumin induced a significant increase in the ROS levels. Similarly, Kawai et al (51) noted that while prolonged exposure of vascular smooth muscle cells to glucocorticoids resulted in inhibition of cell proliferation, pulsatile exposure resulted in a proliferative effect. Previous reports also describe the concept of 'metronomic chemotherapy', in which regular, low-dose chemotherapy results in tumor growth suppression through inhibition of angiogenesis (52, 53). This is different from conventional high-dose, cyclical chemotherapy, which results in direct killing of cancer cells. Based on the sustained, near-constant blood levels of curcumin achieved with microparticles compared to the peaks and troughs observed with repeated IP dosing and the significant inhibition of angiogenesis observed only with microparticles, a case could be made for 'metronomic chemoprevention' with microparticles. Further studies are needed to test this possibility.

In conclusion, a single dose of curcumin microparticles resulted in sustained systemic availability of curcumin and inhibited the growth of MDA-MB-231 xenografts. Repeated IP dosing resulted in peaks and troughs in curcumin blood concentrations and was not effective in inhibiting tumor growth. Injectable sustained release formulations may provide a novel, patient-friendly, and clinically translatable approach to cancer chemoprevention.

Acknowledgments

References

1. Thangapazham RL, Sharma A, Maheshwari RK. Multiple molecular targets in cancer chemoprevention by curcumin. Aaps J 2006;8:E443–9. [PubMed: 17025261]

2. Goel A, Kunnumakkara AB, Aggarwal BB. Curcumin as "Curecumin": from kitchen to clinic. Biochem Pharmacol 2008;75:787–809. [PubMed: 17900536]

3. Anand P, Kunnumakkara AB, Newman RA, Aggarwal BB. Bioavailability of curcumin: problems and promises. Mol Pharm 2007;4:807–18. [PubMed: 17999464]

4. Pan MH, Huang TM, Lin JK. Biotransformation of curcumin through reduction and glucuronidation in mice. Drug Metab Dispos 1999;27:486–94. [PubMed: 10101144]

5. Yang KY, Lin LC, Tseng TY, Wang SC, Tsai TH. Oral bioavailability of curcumin in rat and the herbal analysis from Curcuma longa by LC-MS/MS. Journal of chromatography 2007;853:183–9. [PubMed: 17400527]

6. Cheng AL, Hsu CH, Lin JK, et al. Phase I clinical trial of curcumin, a chemopreventive agent, in patients with high-risk or pre-malignant lesions. Anticancer Res 2001;21:2895–900. [PubMed: 11712783]

7. Sharma RA, Euden SA, Platton SL, et al. Phase I clinical trial of oral curcumin: biomarkers of systemic activity and compliance. Clin Cancer Res 2004;10:6847–54. [PubMed: 15501961]

8. Garcea G, Jones DJ, Singh R, et al. Detection of curcumin and its metabolites in hepatic tissue and portal blood of patients following oral administration. Br J Cancer 2004;90:1011–5. [PubMed: 14997198]

9. Singletary K, MacDonald C, Wallig M, Fisher C. Inhibition of 7,12-dimethylbenz[a]anthracene (DMBA)-induced mammary tumorigenesis and DMBA-DNA adduct formation by curcumin. Cancer Lett 1996;103:137–41. [PubMed: 8635149]

10. Li L, Braiteh FS, Kurzrock R. Liposome-encapsulated curcumin: in vitro and in vivo effects on proliferation, apoptosis, signaling, and angiogenesis. Cancer 2005;104:1322–31. [PubMed: 16092118]

11. Bodmeier R, McGinity JW. The preparation and evaluation of drug-containing poly(dl-lactide) microspheres formed by the solvent evaporation method. Pharm Res 1987;4:465–71. [PubMed: 3508558]

12. Wang YM, Sato H, Horikoshi I. Preparation and characterization of poly(lactic-co-glycolic acid) microspheres for targeted delivery of a novel anticancer agent taxol. Chem Phar Bull 1997;44:1935–40.

13. Zolnik BS, Burgess DJ. Evaluation of in vivo-in vitro release of dexamethasone from PLGA microspheres. J Control Release 2008;127:137–45. [PubMed: 18282629]

14. Kunnumakkara AB, Diagaradjane P, Anand P, et al. Curcumin sensitizes human colorectal cancer to capecitabine by modulation of cyclin D1, COX-2, MMP-9, VEGF and CXCR4 expression in an orthotopic mouse model. Int J Cancer 2009;125:2187–97. [PubMed: 19623659]

15. Kunnumakkara AB, Diagaradjane P, Guha S, et al. Curcumin sensitizes human colorectal cancer xenografts in nude mice to gamma-radiation by targeting nuclear factor-kappaB-regulated gene products. Clin Cancer Res 2008;14:2128–36. [PubMed: 18381954]

16. Hasan J, Byers R, Jayson GC. Intra-tumoural microvessel density in human solid tumours. Br J Cancer 2002;86:1566–77. [PubMed: 12085206]

17. Sapino A, Bongiovanni M, Cassoni P, et al. Expression of CD31 by cells of extensive ductal in situ and invasive carcinomas of the breast. J Pathol 2001;194:254–61. [PubMed: 11400156]

18. Bachmeier B, Nerlich AG, Iancu CM, et al. The chemopreventive polyphenol Curcumin prevents hematogenous breast cancer metastases in immunodeficient mice. Cell Physiol Biochem 2007;19:137–52. [PubMed: 17310108]

19. Aggarwal BB, Shishodia S, Takada Y, et al. Curcumin suppresses the paclitaxel-induced nuclear factor-kappaB pathway in breast cancer cells and inhibits lung metastasis of human breast cancer in nude mice. Clin Cancer Res 2005;11:7490–8. [PubMed: 16243823]

20. Trihia H, Murray S, Price K, et al. Ki-67 expression in breast carcinoma: its association with grading systems, clinical parameters, and other prognostic factors--a surrogate marker? Cancer 2003;97:1321–31. [PubMed: 12599241]

21. Davis CD, Milner JA. Biomarkers for diet and cancer prevention research: potentials and challenges. Acta Pharmacol Sin 2007;28:1262–73. [PubMed: 17723162]

22. Lopez-Lazaro M. Anticancer and carcinogenic properties of curcumin: considerations for its clinical development as a cancer chemopreventive and chemotherapeutic agent. Mol Nutr Food Res 2008;52 (Suppl 1):S103–27. [PubMed: 18496811]

23. Howells LM, Moiseeva EP, Neal CP, et al. Predicting the physiological relevance of in vitro cancer preventive activities of phytochemicals. Acta Pharmacol Sin 2007;28:1274–304. [PubMed: 17723163]

24. Ahmann FR, Citrin DL, deHaan HA, et al. Zoladex: a sustained-release, monthly luteinizing hormone-releasing hormone analogue for the treatment of advanced prostate cancer. J Clin Oncol 1987;5:912–7. [PubMed: 2953870]

25. Minkov NK, Zozikov BI, Yaneva Z, Uldry PA. A phase II trial with new triptorelin sustained release formulations in prostatic carcinoma. Int Urol Nephrol 2001;33:379–83. [PubMed: 12092661]

26. Sastre RL, Olmo R, Teijon C, Muniz E, Teijon JM, Blanco MD. 5-Fluorouracil plasma levels and biodegradation of subcutaneously injected drug-loaded microspheres prepared by spray-drying poly

(D,L-lactide) and poly(D,L-lactide-co-glycolide) polymers. Int J Pharm 2007;338:180–90. [PubMed: 17336474]

27. Yen SY, Sung KC, Wang JJ, Yoa-Pu Hu O. Controlled release of nalbuphine propionate from biodegradable microspheres: in vitro and in vivo studies. Int J Pharm 2001;220:91–9. [PubMed: 11376971]

28. Wang SH, Zhang LC, Lin F, et al. Controlled release of levonorgestrel from biodegradable poly(D,L-lactide-co-glycolide) microspheres: in vitro and in vivo studies. International J Pharm 2005;301:217–25.

29. Hickey T, Kreutzer D, Burgess DJ, Moussy F. In vivo evaluation of a dexamethasone/PLGA microsphere system designed to suppress the inflammatory tissue response to implantable medical devices. J Biomed Mater Res 2002;61:180–7. [PubMed: 12007197]

30. Orloff LA, Dombb AJ, Teomimb D, Fishbein I, Golomb G. Biodegradable implant strategies for inhibition of restenosis. Adv Drug Deliv Rev 1997;24:3–9.

31. Shive MS, Anderson JM. Biodegradation and biocompatibility of PLA and PLGA microspheres. Adv Drug Deliv Rev 1997;28:5–24. [PubMed: 10837562]

32. Chainani-Wu N. Safety and anti-inflammatory activity of curcumin: a component of tumeric (Curcuma longa). J Altern Complement Med 2003;9:161–8. [PubMed: 12676044]

33. Hong J, Bose M, Ju J, et al. Modulation of arachidonic acid metabolism by curcumin and related beta-diketone derivatives: effects on cytosolic phospholipase A(2), cyclooxygenases and 5-lipoxygenase. Carcinogenesis 2004;25:1671–9. [PubMed: 15073046]

34. Skrzypczak-Jankun E, McCabe NP, Selman SH, Jankun J. Curcumin inhibits lipoxygenase by binding to its central cavity: theoretical and X-ray evidence. Int J Mol Med 2000;6:521–6. [PubMed: 11029517]

35. Zhang LJ, Wu CF, Meng XL, et al. Comparison of inhibitory potency of three different curcuminoid pigments on nitric oxide and tumor necrosis factor production of rat primary microglia induced by lipopolysaccharide. Neurosci Lett 2008;447:48–53. [PubMed: 18838107]

36. Khor TO, Keum YS, Lin W, et al. Combined inhibitory effects of curcumin and phenethyl isothiocyanate on the growth of human PC-3 prostate xenografts in immunodeficient mice. Cancer Res 2006;66:613–21. [PubMed: 16423986]

37. Wischke C, Schwendeman SP. Principles of encapsulating hydrophobic drugs in PLA/PLGA microparticles. Int J Pharm 2008;364:298–327. [PubMed: 18621492]

38. Alexis AF. Factors affecting the degradation and drug release mechanism of poly(lactic) acid and poly [(lactic acid)-co-(glycolic acid)]. Polymer International 2005;54:36–46.

39. Lee YT. Breast carcinoma: pattern of metastasis at autopsy. J Surg Oncol 1983;23:175–80. [PubMed: 6345937]

40. Weigelt B, Peterse JL, van 't Veer LJ. Breast cancer metastasis: markers and models. Nat Rev Cancer 2005;5:591–602. [PubMed: 16056258]

41. Shankar S, Ganapathy S, Chen Q, Srivastava RK. Curcumin sensitizes TRAIL-resistant xenografts: molecular mechanisms of apoptosis, metastasis and angiogenesis. Mol Cancer 2008;7:16. [PubMed: 18226269]

42. Williams CS, Mann M, DuBois RN. The role of cyclooxygenases in inflammation, cancer, and development. Oncogene 1999;18:7908–16. [PubMed: 10630643]

43. Plummer SM, Holloway KA, Manson MM, et al. Inhibition of cyclo-oxygenase 2 expression in colon cells by the chemopreventive agent curcumin involves inhibition of NF-kappaB activation via the NIK/IKK signalling complex. Oncogene 1999;18:6013–20. [PubMed: 10557090]

44. Baldin V, Lukas J, Marcote MJ, Pagano M, Draetta G. Cyclin D1 is a nuclear protein required for cell cycle progression in G1. Genes & development 1993;7:812–21. [PubMed: 8491378]

45. Shishodia S, Amin HM, Lai R, Aggarwal BB. Curcumin (diferuloylmethane) inhibits constitutive NF-kappaB activation, induces G1/S arrest, suppresses proliferation, and induces apoptosis in mantle cell lymphoma. Biochem Pharmacol 2005;70:700–13. [PubMed: 16023083]

46. Mukhopadhyay A, Banerjee S, Stafford LJ, Xia C, Liu M, Aggarwal BB. Curcumin-induced suppression of cell proliferation correlates with down-regulation of cyclin D1 expression and CDK4-mediated retinoblastoma protein phosphorylation. Oncogene 2002;21:8852–61. [PubMed: 12483537]

47. Singh M, Singh N. Molecular mechanism of curcumin induced cytotoxicity in human cervical carcinoma cells. Mol Cell Biochem 2009;325:107–19. [PubMed: 19191010]

48. Thayyullathil F, Chathoth S, Hago A, Patel M, Galadari S. Rapid reactive oxygen species (ROS) generation induced by curcumin leads to caspase-dependent and -independent apoptosis in L929 cells. Free Radic Biol Med 2008;45:1403–12. [PubMed: 18762247]

49. Aggarwal S, Ichikawa H, Takada Y, Sandur SK, Shishodia S, Aggarwal BB. Curcumin (diferuloylmethane) down-regulates expression of cell proliferation and antiapoptotic and metastatic gene products through suppression of IkappaBalpha kinase and Akt activation. Mol Pharmacol 2006;69:195–206. [PubMed: 16219905]

50. Kang J, Chen J, Shi Y, Jia J, Zhang Y. Curcumin-induced histone hypoacetylation: the role of reactive oxygen species. Biochem Pharmacol 2005;69:1205–13. [PubMed: 15794941]

51. Kawai Y, Hayashi T, Eguchi K, et al. Effects of brief glucocorticoid exposure on growth of vascular smooth muscle cells in culture. Biochem Biophys Res Commun 1998;245:493–6. [PubMed: 9571182]

52. Bertolini F, Paul S, Mancuso P, et al. Maximum tolerable dose and low-dose metronomic chemotherapy have opposite effects on the mobilization and viability of circulating endothelial progenitor cells. Cancer Res 2003;63:4342–6. [PubMed: 12907602]

53. Kerbel RS, Kamen BA. The anti-angiogenic basis of metronomic chemotherapy. Nat Rev Cancer 2004;4:423–36. [PubMed: 15170445]
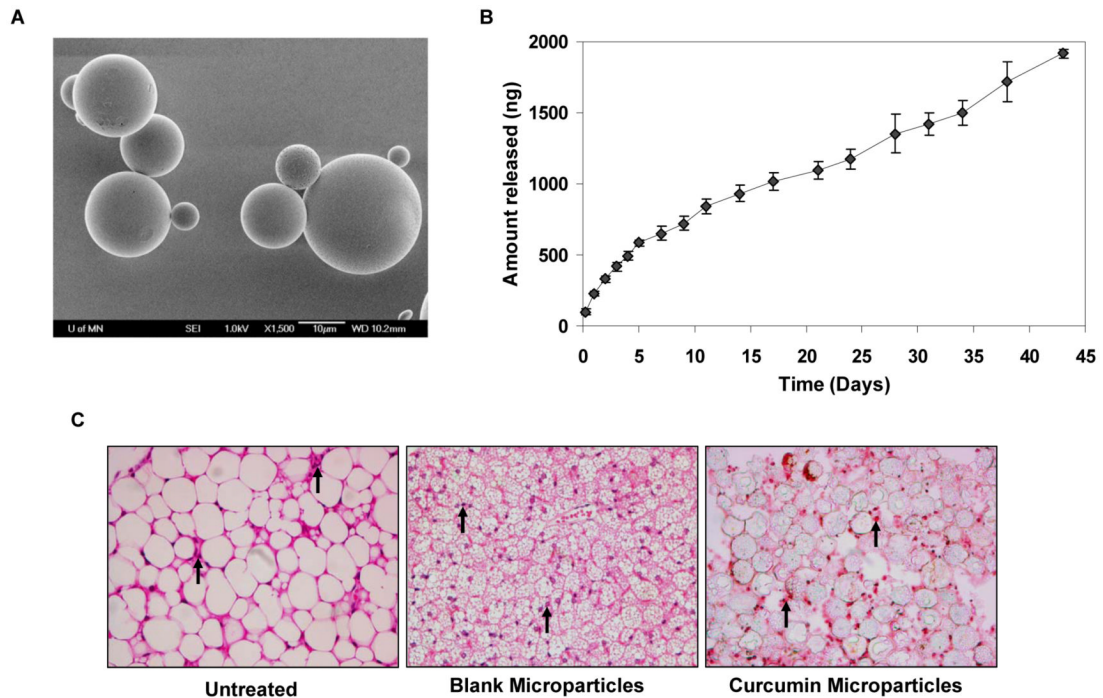
Figure 1.
A, SEM image of curcumin-loaded PLGA microparticles. Microparticles were placed on a double stick tape and carbon coated before observation under an electron microscope. 1500X magnification. Bar is 10 μm. *B, In vitro* release of curcumin from microparticles. Microparticles (equivalent to 2 μg of curcumin), suspended in 1 ml release buffer, were added on top of the Transwell® insert and 3 ml release buffer was added to the bottom of the well. The bottom chamber was sampled at different time intervals. Curcumin concentrations were quantified by HPLC. Data shown is mean ± SD, n=3. *C,* H & E staining of subcutaneous tissues from the vicinity of the injection site (left – untreated; middle – blank microparticle treated; and right - curcumin microparticle treated). Arrows indicate inflammatory cells. 400X magnification.
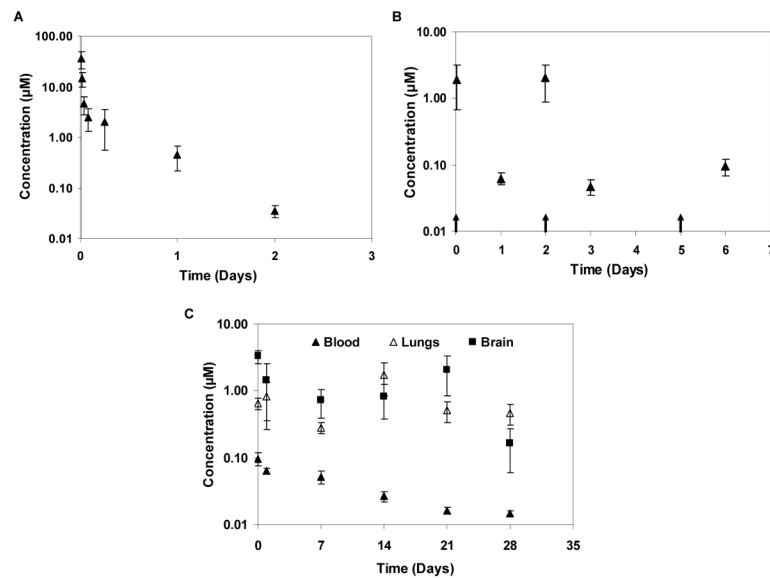
Figure 2.
A, Concentration-time profile of curcumin in blood following a single IP injection of curcumin (2.2 mg) dissolved in 0.05 ml 50/50 PEG 400 and 95% ethanol mixture. Curcumin concentrations were determined by LC-MS/MS. Data shown is mean ± S.E.M., n=6. *B,* Curcumin kinetics following three IP injections of curcumin (2.2 mg curcumin/dose). Arrows indicate times of curcumin dosing. Data shown is mean ± S.E.M., n=6-9. *C,* Curcumin kinetics following a single subcutaneous dose of curcumin microparticles. Microparticles (equivalent to 29.1 mg curcumin) were dispersed in 0.5 ml PBS and injected subcutaneously. Data shown is mean ± S.E.M., n=6-7.
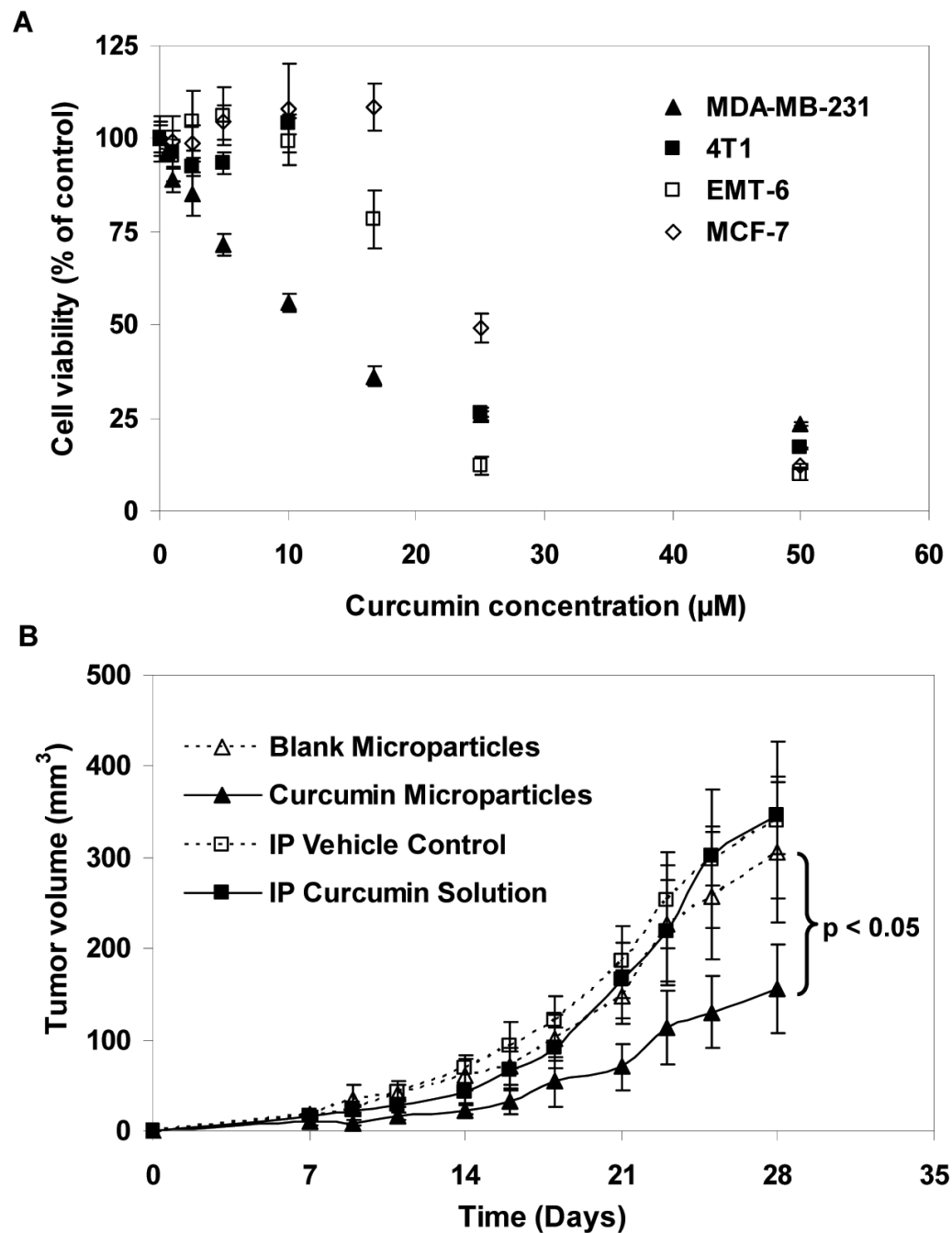
Figure 3.
A, Curcumin cytotoxicity in different breast cancer cell lines. Cells were treated with 0.1-50 µM curcumin for 72 h. Cell viability was measured using MTS assay, and the results were expressed as percent viability relative to control. Data shown is mean ± S.E.M., n=6. *B,* A single dose of curcumin microparticles inhibits MDA-MB-231 tumors. Microparticles (equivalent to 58.2 mg curcumin) were dispersed in 1 ml PBS and injected subcutaneously. For IP doses, curcumin (4.4 mg) was dissolved in 0.1 ml of 75/25 PEG 400 and 95% ethanol mixture and injected thrice a week. Treatments were started one day before the injection of tumor cells. Data shown is mean ± S.E.M., n=6. $p < 0.05$, linear mixed effect ANOVA.
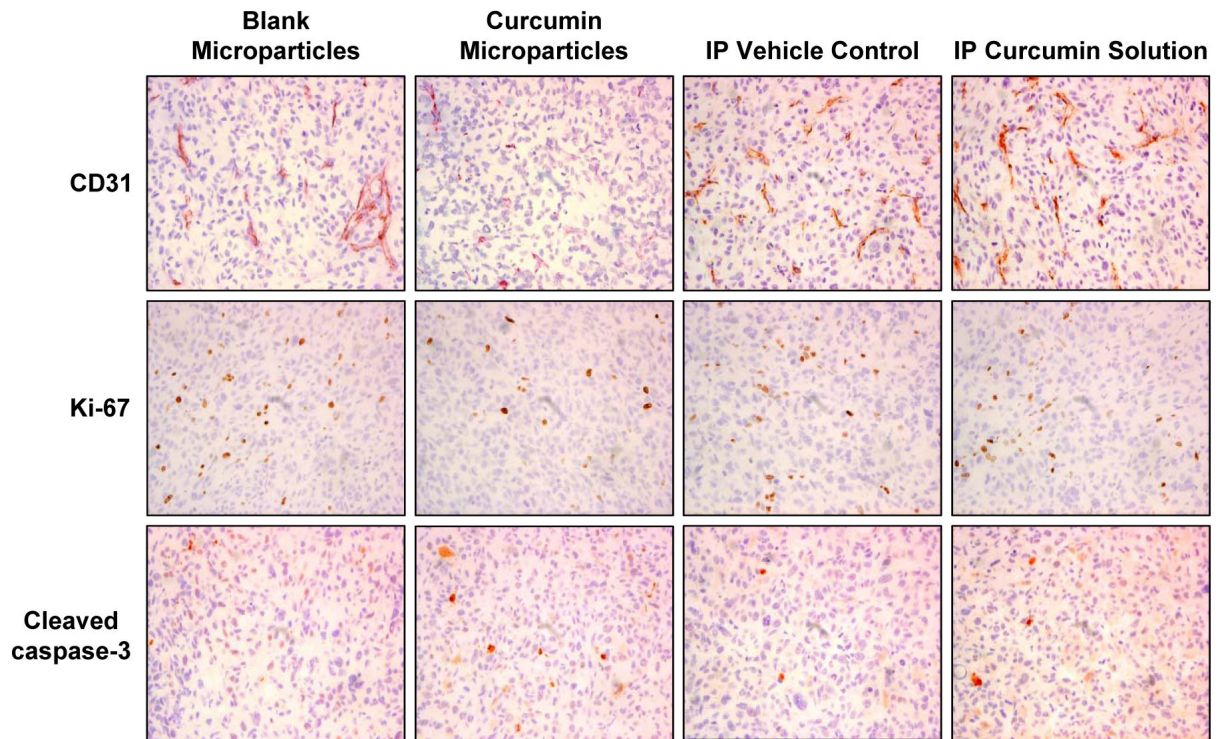
Figure 4.
Effect of curcumin treatment on tumor microvessels, proliferation, and apoptosis. Tumor samples from the *in vivo* efficacy study were sectioned and stained for CD31 (top row), Ki-67 (middle row) and cleaved caspase-3 (bottom row). Tumors from three animals in each group were analyzed and representative images are shown. Cells in the central necrotic region of the tumors were excluded from analysis. 400X magnification.
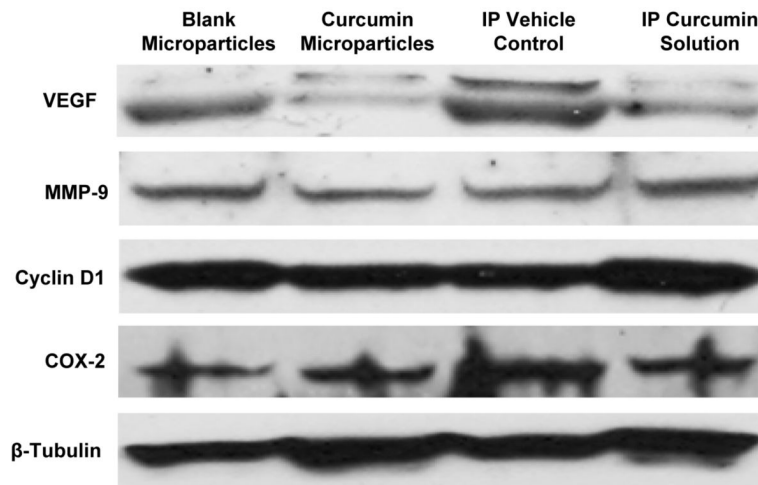
Figure 5.
Effect of curcumin treatment on VEGF, MMP-9, Cyclin D1, and COX-2 expression. Tumor samples from the *in vivo* efficacy study were analyzed for protein expression by Western blotting. β-Tubulin served as the protein loading control.